

Synthesis and comparative study on phase transition behavior of triazole-cored liquid crystals armed with cholesterol and double or triple aromatic rings systems†

Cite this: *New J. Chem.*, 2013, 37, 1906

Guan-Yeow Yeap,^{*a} Subramanian Balamurugan,^a Murugesan Vijay Srinivasan^b and Palaninathan Kannan^b

Two homologous series of optically active bent-shaped mesogens comprising a cholesterol unit as one of the side arms connected to a 1,2,3-triazole ring while the other arm of the triazole ring is connected to two- and three-ring aromatic systems with varying terminal chain lengths have been synthesized. The molecular structure, thermal and optical activities have been studied extensively in which the compounds from both series exhibit polymorphism ranging from chiral nematic (N*), chiral smectic A (SmA*), chiral smectic C (SmC*) and twist grain boundary (TGBC*) phases. A further comparison between the two series of target compounds has drawn a common remark of which the phase behavior is found to be dependent on the length of the terminal tail and number of aromatic rings in the mesogenic units.

Received (in Montpellier, France)
13th January 2013,
Accepted 11th March 2013

DOI: 10.1039/c3nj00053b

www.rsc.org/njc

1. Introduction

Since the discovery of chiral anisotropic fluid phases formed by chiral mesogens or induced by chiral dopants, materials with optically active properties have continued to attract attention from researchers.¹ The molecular chirality is inclined to self-organize leading to the formation of helical structures in a chiral phase.^{2,3} It has been claimed that the helical structure of the molecule can produce chiral nematic (N*), chiral smectic C (SmC*), chiral smectic A (SmA*) and frustrated LC phases such as blue phase and twist grain boundary (TGB). Each of these chiral phases possess potential applications. For instance, the N* phase has been exploited in optical and thermal sensing device applications.^{4–7} The SmC* and SmA* phases formed by chiral mesogens have been well-exploited in electro-optical and spatial light modulation applications, respectively,⁸ and the frustrated blue phase has been studied extensively to determine their potential for the use as media in advanced technology. In the midst of searching for new applications, the studies on TGB

phases has also received great attention. There are three main types of TGB phases including the TGBA, TGBC and TGBC* wherein the smectic order is of orthogonal SmA, SmC and helical SmC*, respectively.⁷

The design of chiral liquid crystalline materials requires the selection of a core, linking groups and terminal functionalities.⁹ Since the term 'click' reaction was reported, it has gained a great deal of attention owing to its high specificity and quantitative yields.¹⁰ Among the 'click' chemistry reactions, the Huisgen dipolar cycloaddition reaction between an azide and an alkyne leading to the formation of 1,2,3-triazole was claimed to be the most convenient method adopted by researchers.¹¹ The importance of this reaction for researchers working on liquid crystals can be rationalized by the presence of the heteroatoms, which are found to be more polarizable than carbon atoms and can promote the desired physical and chemical changes.¹² Recently, Gimeno and co-workers reported that the presence of a 1,2,3-triazole ring would promote well-built intermolecular interactions.¹³

Although attempts to obtain 1,2,3-triazole-based liquid crystals have extensively been carried out in recent years,^{13–15} the formation of 1,2,3-triazole derivatives armed with cholesterol group has rarely been reported. Hence, we report in this paper a new class of low molar mass mesogens derived from cholesterol which represents an exemplary and emerging class of chiral liquid crystals. The cholesterol unit is linked with the

^a Liquid Crystal Research Laboratory, School of Chemical Sciences, Universiti Sains Malaysia, 11800 Minden, Penang, Malaysia.

E-mail: gyeap@usm.my; Fax: +60-4-6574854

^b Department of Chemistry, Anna University, Chennai 600-025, Tamil Nadu, India

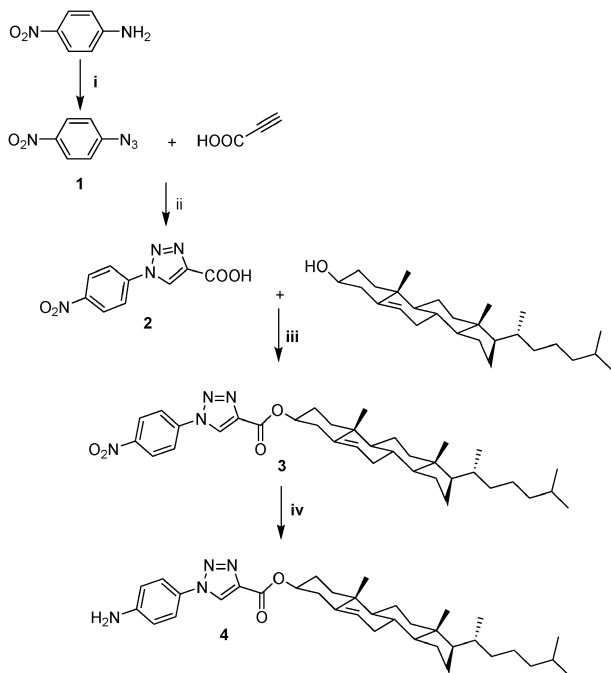
† Electronic supplementary information (ESI) available: Full experimental details, including the general procedure for the synthesis of intermediate and final compounds. See DOI: 10.1039/c3nj00053b

mesogenic units through the 1,2,3-triazole ring. Two series of target compounds are designed wherein the 1,2,3-triazole ring serves as a linking group situated between a cholesterol and a mesogenic unit. The first series contains the mesogenic unit with two aromatic ring while the latter series consists of three rings in the same unit. For both series, the alkyl group C_nH_{2n+1} (where $n = 6$ to 12) is employed as terminal chain attached to the mesogenic unit.

2. Experimental

2.1 Synthesis and characterization

The new class of 1,2,3-triazole containing compounds (series 1 and 2) were prepared using the method summarized in Schemes 1 and 2. 4-Azidonitrobenzene (**1**) was prepared from 4-nitroaniline by a known diazotization method.¹⁴ The azide was reacted with propiolic acid using CuI as a catalyst to obtain 1-(4-nitrophenyl)-1*H*-1,2,3-triazole-4-carboxylic acid (**2**). The esterification of compound **2** with commercially available cholesterol in the presence of DCC and DMAP to yield cholesteryl(1-(4-nitrophenyl)-1*H*-1,2,3-triazole-4-carboxylate) (**3**). The nitro group of compound **3** was reduced by iron powder and ammonium chloride to obtain cholesteryl(1-(4-amino-phenyl)-1*H*-1,2,3-triazole-4-carboxylate) (**4**). The acid catalyzed condensation of compound **4** with 4-*n*-alkyloxybenzaldehyde (**5a–5g**) or 4-(4-*n*-alkyloxybenzoyloxy)-benzaldehyde (**8a–8g**) in ethanol gave the target compounds in reasonably good yields. The detailed synthetic procedures and characterization data for all the compounds are given in the ESI† under the experimental section.



Scheme 1 Reagents and conditions: (i) HCl, NaNO₂, NaN₃; (ii) CuI, THF, N₂ atm; (iii) DCC, DMAP, CH₂Cl₂; (iv) Fe powder, NH₄Cl, ethanol; (v) DCC, DMAP, CH₂Cl₂; (vi) HCl, ethanol.

The phase transition behavior of both series was evaluated using polarizing optical microscopy (POM) and differential scanning calorimetry (DSC). The sample was sandwiched between a clean untreated glass slide and a cover slip. The planar and homeotropically aligned cells were employed in order to substantiate the mesophase. The details of these studies will be discussed in the following section.

3. Results and discussion

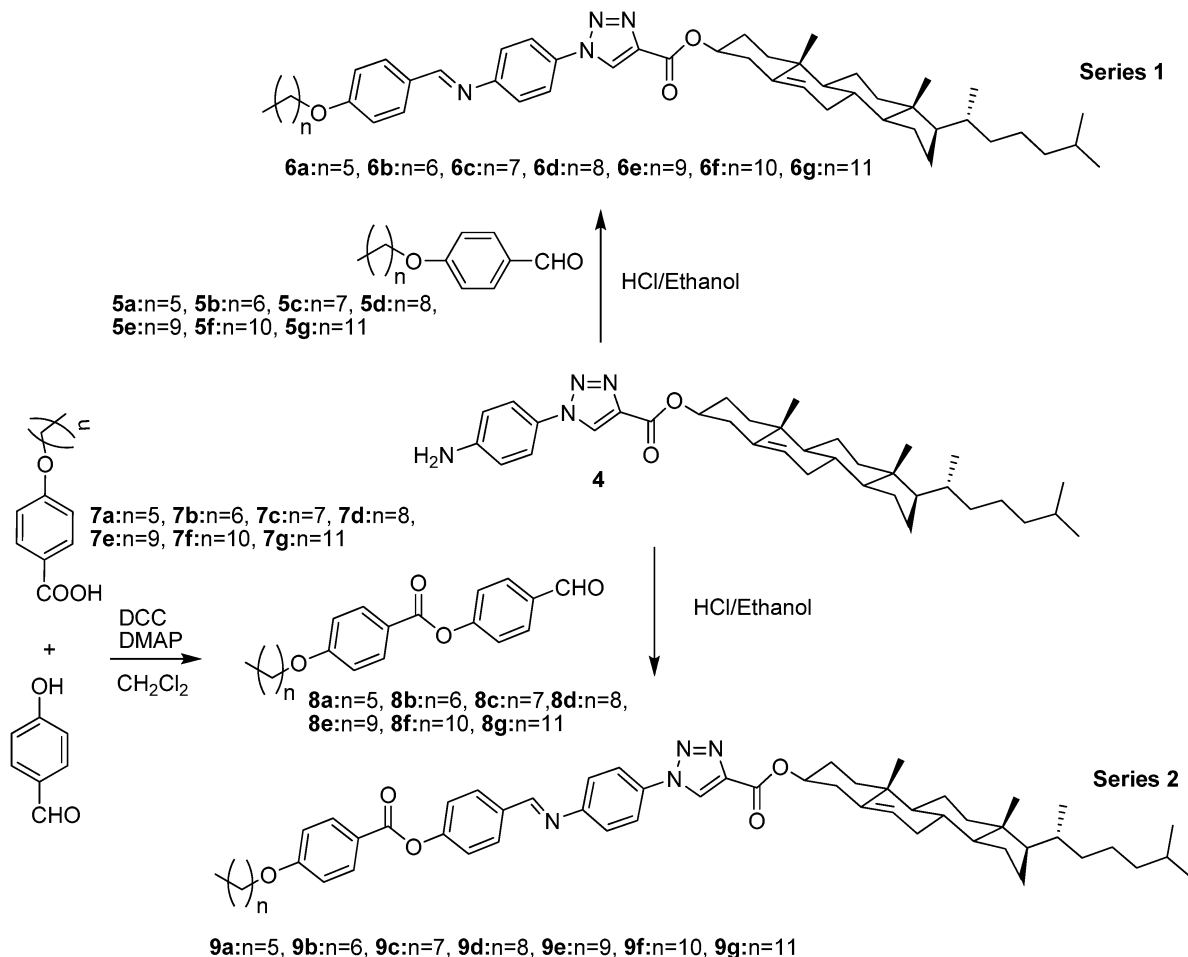
3.1 Microscopic and calorimetric studies of intermediates **3** and **4**

The target bent shaped compounds of series 1 and 2 are obtained from the intermediates with NO₂ and NH₂ functionalized compounds **3** and **4**, respectively. Both of these compounds **3** and **4** also consist of cholesterol group and hence are chiral. It is apparent that compound **3** shows the phase sequence Cr–SmA–I on heating and these transitions are reversible on cooling. However, compound **4** is found to be non-mesogenic (Table 1). The difference between compound **3** and **4** merely lies on the terminal substituent of NO₂ and NH₂ of which the earlier possesses higher clearing point (327 °C) than the latter (230 °C).

3.2 Microscopic and calorimetric studies of compounds **6a–6g**

The compounds **6a–6g** possess a 1,2,3-triazole ring as a central core armed with promesogen cholesterol and another arm made up from two aromatic rings attached by terminal chains of C_nH_{2n+1} where n ranges from 6 to 12. The phase transition behaviors for **6a–6g** are summarized in Table 2. It is apparent from Table 1 that compounds **6a–6g** have very high thermal stabilities as indicated by the high clearing temperatures. For **6a**, however, there was partial thermal decomposition at 290 °C before it turned into an isotropic liquid. As for the compounds **6b–6g**, they possess decomposition temperatures close to the isotropic temperature. These results indicate that the compounds possess high mesophase stability.

In general, the chiral liquid crystal material can induce the cholesteric phase wherein at zero field it exhibits two optical contrasting stable states with planar (oily streak and fingerprint) texture and focal conic texture. As such, most of the mesophase can be identified according to the typical optical textures. From the POM observation the compounds **6a–6g** exhibit cholesteric oily streak texture on heating cycle since the compounds are of high viscous nature. Generally, the calamitic liquid crystals of lower members are nematic, the medium members show nematic and smectic and higher members are merely smectic in nature.¹⁶ The generalization is applicable for this series. The lower homologues **6a** and **6b** show chiral nematic (N*) phase, the medium member of **6c** exhibits N* and SmC phase and the higher homologues **6d–6g** show SmA and/or SmC phase. For compound **6a**, it exhibits typical cholesteric oily streak texture on heating but decomposes before isotropization. Whereas the compound **6b** placed between two ordinary glass slides upon heating shows oily streak texture (Fig. 1a) characteristics of cholesteric phase and the N* phase appears with a focal



Scheme 2 Synthetic pathway of series 1 and 2.

Table 1 Phase transition temperatures (°C) and associated enthalpies [kJ mol⁻¹] for intermediates **3** and **4**

Compound	R	Phase transitions (°C)		
		Heating		Cooling
3	NO ₂	Cr 296 [55.3]	SmA 327 ^a	I 320 ^a SmA 288 [48.6] Cr
4	NH ₂	Cr 230 [78.7]	I	I 209 [67.2] Cr

Phase transition temperatures were determined by DSC thermogram. Abbreviations: Cr = crystal, SmA* = chiral smectic A phase; I = isotropic phase. ^a Data obtained by POM.

conic texture upon cooling. The focal conic texture transformed to planar texture having oily streak (Fig. 1b) by shearing the mesophase.

The compound **6c** shows polymorphism on cooling from the isotropic liquid and the phase sequence is found as Iso-N*-SmA*-Cr. For this compound, on cooling from isotropic phase exhibits N* phase with planar fingerprint texture (Fig. 2a). The fingerprint texture was regained when it was applied with

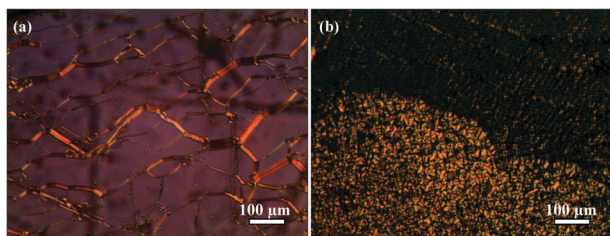
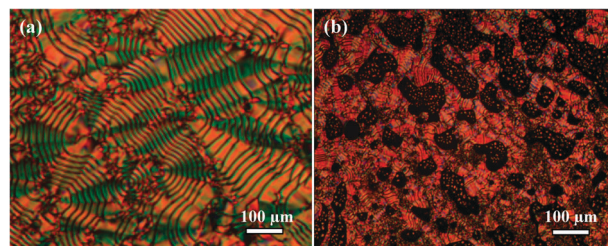
the mechanical stress indicating the long pitch of the N* phase. On further cooling the N* phase changed to SmA* phase (Fig. 2b) through the formation of both striking focal-conic and pseudoisotropic textures. The SmA* phase was confirmed by the sample subjected to homeotropically treated cell which shows a characteristic focal conic texture and a dark field of view (Fig. 2c). Finally the compound **6c** crystallized at 172 °C.

The remaining members of **6d-6f** exhibit the phase transition sequence of I-SmA*-SmC*-Cr. These compounds display typical cholesteric oily streak texture on heating. In order to clarify further, the discussion will be based on a representative compound **6f**. The compound **6f** exhibits the monotropic SmA* and SmC* phases. The focal conic texture appears as a pseudoisotropic pattern typical of the SmA phase when the sample placed between homogeneously treated thin cell with a gap of $d = 5 \pm 0.2 \mu\text{m}$. On further cooling the sample SmC* phase appears as nucleating batonnets superimposed by the equidistant patterns as shown in Fig. 3a. On further cooling the sample crystallized at 157 °C. The last member of the series **6g** exhibits usual oily streaks texture on heating cycle and SmC* phase (Fig. 3b) was observed on cooling from the isotropic liquid.

Table 2 Phase transition temperatures (°C) and associated enthalpies [kJ mol⁻¹] for compounds **6a–6g**

Compound	Phase sequence		
	<i>n</i>	Heating	Cooling
6a	5	Cr 184 [54.1] N* 290 ^b I	—
6b	6	Cr 183 [68.7] Ch 288 [18.6] I	I 285 [17.8] N* 179 ^a Cr
6c	7	Cr 180 [47.9] Ch 295 [12.0] I	I 290 [10.6] N* 257 ^c SmA* 172 [24.8] Cr
6d	8	Cr 175 [22.3] Ch 260 [22.3] I	I 255 [8.5] SmA* 213 ^c SmC*161 [14.6] Cr
6e	9	Cr 171 [42.7] Ch 257 [17.4] I	I 256 [13.7] SmA* 222 [5.3] SmC* 158 [29.5] Cr
6f	10	Cr 166 [35.6] Ch 255 ^c I	I 250 [9.8] SmA* 249 ^c SmC*157 [24.2] Cr
6g	11	Cr 131 [41.5] Ch 258 ^c I	I 253 [26.4] SmC* 125 ^c Cr

Phase transition temperatures were determined by DSC thermogram. Abbreviations: Cr = crystal, Ch = cholestric phase; N* = chiral nematic phase; SmA* = chiral smectic A phase; TGBC* = twist grain boundary phase with SmC* blocks; I = isotropic phase. ^a Data obtained by POM. ^b A partial decomposition of the material at the isotropic liquid was detected by POM. ^c Phase transition was weak and could only be observed under POM.

**Fig. 1** Photomicrographs of the textures of compound **6a**: (a) oily streak texture of the N* phase at 243 °C, and (b) planar texture of N* transformation for focal conic texture on subjected to mechanical stress at 269 °C.**Fig. 3** Photomicrographs of the textures (a) SmC* phase (243 °C) of compound **6f** seen from the homeotropically treated cell, and (b) planar SmC* phase appearing just below the isotropic phase of the compound **6g**.

3.3 Microscopic and calorimetric studies of compounds **9a–9g**

In this series the 1,2,3-triazole ring connected with a cholesterol unit in one arm and another arm comprises of three aromatic ring attached by terminal alkyl chain of C_nH_{2n+1} where *n* ranges from 6 to 12. The phase transition behaviors of the compounds **9a–9g** are summarized in Table 3. All homologues in this series display enantiotropic mesomorphism. The first member **9a** displays oily streak texture of chiral nematic phase while cooling from the isotropic phase. The N* phase with a focal conic texture is changed to oily streak (Grandjean planar) texture when it was subjected to mechanical stress. Further cooling the N* phase has led to TGBC* phase by the planar pattern in a homogeneous glass slides (Fig. 4a). When the

sample is subjected to the homeotropic alignment it displays filamentary pattern of the TGBC* phase (Fig. 4b).

Similarly the compound **9b** exhibits N* phase on cooling from the isotropic state and further cooling, the TGBC* phase appeared as a filament texture which is stable over a temperature range of 13 °C. The presence of TGBC* phase indicates that the compound is strongly chiral and thus the pitch of their N* phase is shorter. The other member of **9c** exhibits a chiral oily streak pattern on heating cycle and upon cooling focal conic texture was observed. The focal conic texture was destroyed and Grandjean planar texture formed when a gentle shearing was applied on the glass plate. The observation is a characteristic of the unique nature of N*

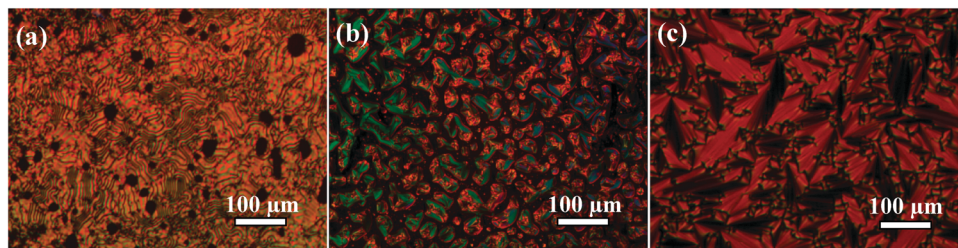
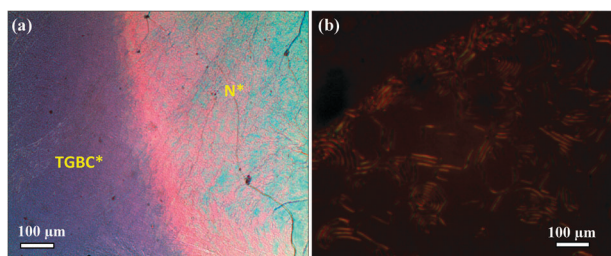
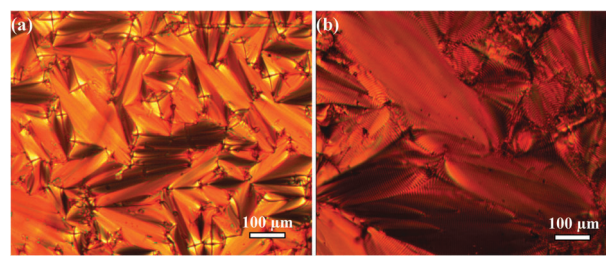
**Fig. 2** Photomicrographs of the textures observed for different mesophase of compound **6c**: (a) the planar finger print texture of the N* phase at 285 °C, (b) focal conic texture of the SmA* phase at 185 °C, and (c) focal conic texture of SmA phase in homogeneously aligned cell.

Table 3 Phase transition temperatures (°C) and associated enthalpies [kJ mol⁻¹] for compounds **9a–9g**

Compound	<i>n</i>	Phase sequence	
		Heating	Cooling
9a	5	Cr 148 [33.5] N* 271 [4.7] I	I 266 [4.5] N* 150 ^a TGBC* 143 [25.8] Cr
9b	6	Cr 145 [29.1] N* 269 [8.2] I	I 265 [7.7] N* 155 ^a TGBC* 142 [22.6] Cr
9c	7	Cr 144 [43.6] N* 266 [11.3] I	I 259 [11.0] N* 141 [31.5] Cr
9d	8	Cr 140 [20.7] SmA* 261 [6.6] I	I 257 [5.9] SmA* 137 [20.0] Cr
9e	9	Cr 163 [26.1] SmA* 278 [7.2] I	I 266 SmA* 158 ^b Cr
9f	10	Cr 160 [36.5] SmC* 216 ^a SmA 260 [4.5] I	I 252 [4.1] SmA* 210 ^a SmC* 156 [36.2] Cr
9g	11	Cr 158 [18.7] SmC* 232 ^a SmA 258 [9.4] I	I 255 [8.8] SmA* 224 ^a SmC* 153 [18.4] Cr

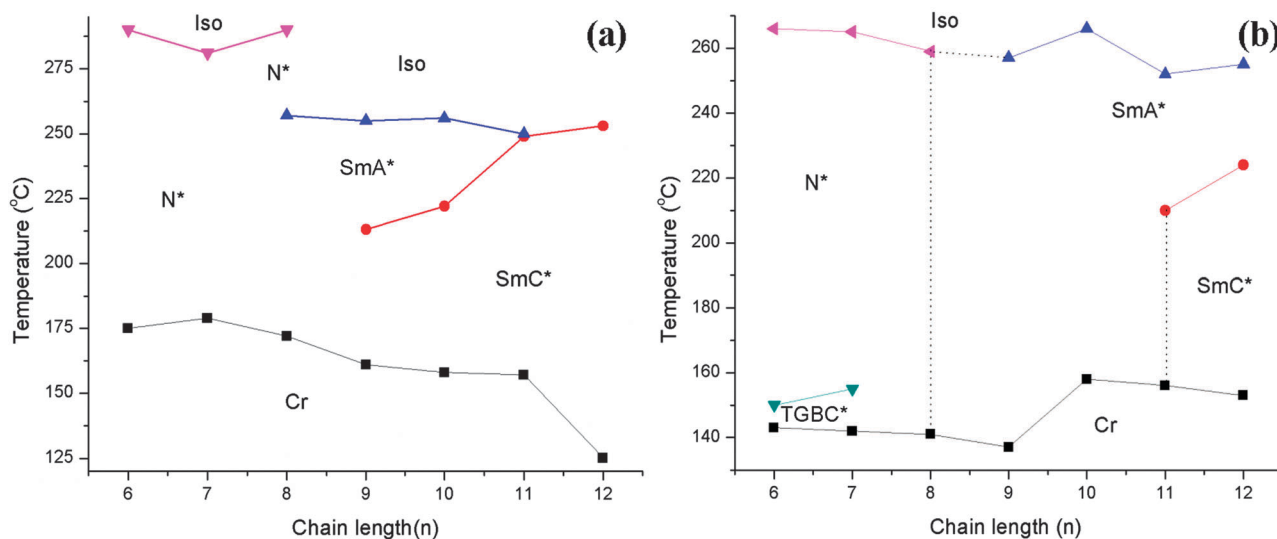
Phase transition temperatures were determined by DSC thermogram. Abbreviations: Cr = crystal, Ch = cholesteric phase; N* = chiral nematic phase; SmA* = chiral smectic A phase; TGB = twist grin boundary phase with SmC* blocks; I = isotropic phase. ^a Data obtained by POM. ^b Phase transition was weak and could only be observed under POM.

**Fig. 4** Photomicrographs of the texture of compound **9a**. (a) Phase transformation from N* to TGBC* (150 °C) and (b) filamentary texture of the homeotropically aligned TGBC* phase (148 °C).**Fig. 5** Photomicrographs of the texture of compound **9g** phase observed from homeotropically treated cell (a) SmA* phase at 220 °C, and (b) SmC* at 188 °C.

phase. Finally, the compounds **9b** and **9c** crystallized at 145 °C and 151 °C, respectively.

The compounds **9d** and **9e** undergo slow cooling from the isotropic liquid whereupon the SmA* phase was observed at 257 °C and 266 °C, respectively. The discussion on how to

define the textural pattern will be based on compound **9d**. On heating the sample **9d** between the clean glass slides to isotropic liquid and cooling slowly the formation of focal conic fans suggests a layered structure. This SmA* phase was confirmed by unique focal conic texture observed on slides treated for planar orientation and a dark field of view when

**Fig. 6** Correlation between transition temperature and methylene chain length for (a) compound **6a–g** and (b) compound **9a–g**.

subjected to homogeneously treated cell. Finally the compound **9d** crystallized at 137 °C.

The higher homologues **9f** and **9g** exhibit dimesomorphic sequence of I-SmA*–SmC*–Cr under the POM. When the homogeneously treated cell was filled by these compound **9g** and cooled from the isotropic phase, it exhibits a pseudoisotropic pattern characteristics of the SmA* phase. On further cooling to 220 °C the SmA* phase (Fig. 5a) changed to SmC* phase which appears as nucleating batonnets superimposed by the equidistant line pattern (Fig. 5b) at 188 °C. It can also be seen in Fig. 6 which represents the correlation between the transition temperatures and respective terminal chain lengths. The lower homologues of both series exhibit nematic phase while increasing the terminal chain length will lead to the formation of smectic phase. Interestingly, the highly frustrated TGBC* phase prevails in lower homologues of three rings system (series 2). This material could be used as one of the components for preparing mixtures capable of stabilizing TGBC* phase.

Conclusions

Two series of click chemistry assisted cholesterol-based liquid crystals have been synthesized and characterized. In the first series, two aromatic rings are connected to triazole ring; while in second series three aromatic rings are connected to triazole ring. In both series the length of the terminal tail was varied from 6 to 12. The structural factors strongly influence the phase transition behaviour of target compounds. All members of these series show mesomorphism *viz.* mono, di and polymorphism. These mesophases possess very high thermal stability and the isotropic temperature is >250 °C. The lower homologues **6a** and **6b** of the first series exhibits N* phase, the medium homologues **6c** shows dimesomorphic sequence involving the transition from SmA*–N* phase, whereas the higher homologues display the smectic phase SmA* and/or SmC* phase. Interestingly, the lower homologues **9a** and **9b** of the second series exhibited dimesomorphic sequence of N*–TGBC*. The compound **9c** of the medium homologues displayed N* phase, compounds **9d** and **9e** showed SmA* phase, and the higher homologues **9f** and **9g** displayed nucleating batonnet SmC* phase. In both series the smectogenic properties of the compounds increased with increasing terminal chain length.

Acknowledgements

The main author (G-Y. Yeap) would like to thank the Malaysian Ministry of Higher Education or MOHE for the Fundamental Research Grant Scheme (FRGS) no. 203/PKIMIA/6711265. Authors are also grateful to Prof. Masato M. Ito from Soka University for the support of some chemicals from TCI, Japan.

References

- (a) F. Renitzer, *Monatsh. Chem.*, 1888, **9**, 421–441; (b) C. V. Yelamaggad, N. L. Bonde, A. S. Achalkumar, D. S. Shankar Rao, S. Krishna Prasad and A. K. Prajapathi, *Chem. Mater.*, 2007, **19**, 2463–2472.
- (a) M. Marcos, J. L. Serrano, T. Sierra and M. J. Gimenez, *Angew. Chem., Int. Ed. Engl.*, 1992, **31**, 1471–1472; (b) M. J. Baena, J. Barbera, P. Espinet, A. Ezcurra, M. B. Ros and J. L. Serrano, *J. Am. Chem. Soc.*, 1994, **116**, 1899–1906.
- H. Kizerow, in *Chirality in Liquid Crystals*, ed. H. S. Kitzerow and C. Bahr, Springer-Verlag, New York, 2001.
- (a) I. Sage, in *Liquid Crystals. Applications and Uses*, ed. B. Bahadur, World scientific, Singapore, 1992, vol. 3, ch. 20; (b) J. Constant, D. G. McDonnell and E. P. Raynes, *Mol. Cryst. Liq. Cryst.*, 1987, **144**, 161–168.
- D. M. Walba, F. Stevens, N. A. Clark and D. C. Parks, *Acc. Chem. Res.*, 1996, **29**, 591–597.
- (a) P. P. Crooker, *Liq. Cryst.*, 1989, **5**, 751–775; (b) P. P. Crooker, *Mol. Cryst. Liq. Cryst.*, 1983, **98**, 31–45.
- (a) P. J. Collings and J. S. Patel, *Handbook of Liquid Crystal Research*, Oxford University Press, New York, Oxford, 1997; (b) G. Shanker and C. V. Yelamaggad, *New J. Chem.*, 2012, **36**, 918–926; (c) S. Garoff and R. Meyer, *Phys. Rev. Lett.*, 1977, **38**, 848–851.
- S. T. Lagerwall, M. Matuszyk, P. Rodhe and L. Odma, in *The Optics of Thermotropic Liquid Crystals*, ed. S. J. Elston and J. R. Sambles, Taylor and Francis, London, 1998.
- D. Demus, J. Goodby, G. W. Gray, H. W. Spiess and V. Vill, *Handbook of liquid crystals*, Wiley-VCH, New York, 1998, vol. 3.
- (a) H. C. Kolb, M. G. Finn and K. B. Sharpless, *Angew. Chem., Int. Ed.*, 2001, **40**, 2004–2021; (b) Z. P. Demko and K. B. Sharpless, *Angew. Chem., Int. Ed.*, 2002, **41**, 2110–2113; (c) Z. P. Demko and K. B. Sharpless, *Angew. Chem., Int. Ed.*, 2002, **41**, 2113.
- (a) R. Huisgen, G. Szeimies and L. Mobius, *Chem. Ber.*, 1967, **100**, 2494–2507; (b) K. V. Gothelf and K. A. Jorgensen, *Chem. Rev.*, 1998, **98**, 863–909.
- G. Y. Yeap, A. Alshargabi, M. M. Ito, W. A. K. Mahmood and D. Takeuchi, *Mol. Cryst. Liq. Cryst.*, 2012, **557**, 126–133.
- N. Gimeno, R. Martin-Rapun, S. Rodriguez-Conde, J. L. Serrano, C. L. Folcia, M. A. Pericas and M. B. Ros, *J. Mater. Chem.*, 2012, **22**, 16791–16800.
- (a) K. C. Majumdar, S. Mondal and R. K. Sinha, *New J. Chem.*, 2010, **34**, 1255–1260; (b) C. V. Yelamaggad, A. S. Achalkumar, N. L. Bonde and A. K. Prajapathi, *Chem. Mater.*, 2007, **19**, 2463–2472; (c) V. I. Kopp, B. Fan, H. K. M. Vithana and A. Z. Genack, *Opt. Lett.*, 1998, **23**, 1707–1709.
- Z. Cui, Y. Zhang and S. He, *Colloid Polym. Sci.*, 2008, **286**, 1553–1559.
- P. J. Collings and M. Hird, *Introduction to Liquid Crystals Chemistry and Physics*, Taylor and Francis Ltd., London, 1997.

Copyright of New Journal of Chemistry is the property of Royal Society of Chemistry and its content may not be copied or emailed to multiple sites or posted to a listserv without the copyright holder's express written permission. However, users may print, download, or email articles for individual use.